Dynamical Instabilities in Differentially Rotating Stellar Systems

A. L. Varri[1,2], E. Vesperini[2], S. L. W. McMillan[3], G. Bertin[4]

[1] University of Edinburgh (UK) [2] Indiana University (USA) [3] Drexel University (USA) [4] Università degli Studi di Milano (Italy)

Outline

- We study the emergence of dynamical instabilities in stellar dynamical models characterized by a strong degree of differential rotation and relatively low values of the ratio of the rotational kinetic energy to the gravitational energy $t = K_{rot}/|W|$.
- The instabilities are dominated by coherent global modes with azimuthal number $m = 1, 2$. For the relevant unstable modes, corotation occurs inside the rotating configuration.
- Such instabilities show striking similarities with the dynamical instabilities observed in low t differentially rotating fluid polytropes.
- This result represents a first step in the investigation of the analogies between stellar and fluid rotating spheroidal systems in a regime currently unexplored.

Method and initial conditions

We consider the class of axisymmetric rotating equilibria [9] defined by the DF:

$$f_{WT}(I) = A \exp(-aE_0)\{\exp[-a(I - E_0)] - 1 + a(I - E_0)\} \quad (1)$$

if $E \leq E_0$ and $f_{WT}(I) = 0$ otherwise, with $I = E - [\omega J_z/(1 + bJ_z^{2c})]$. The family of self-consistent models is characterized by two main parameters (Ψ, χ), measuring the depth of the central potential well and the central rotation strength, respectively. We consider configurations in the regime of strong differential rotation, that is, such that $0.4 \leq \hat{\omega}/\hat{\omega}_{max} \leq 1.0$, where $\hat{\omega} = 3\chi^{1/2}$ is the central dimensionless angular velocity.

Id	N	Ψ	χ	$\hat{\omega}/\hat{\omega}_{max}$	t	ρ_{max}/ρ_0	σ_1	$\sigma_2/2$
C2R90	65536	2	3.92	0.9	0.16	5.37	2.90	0.75
C2R70	65536	2	2.37	0.7	0.14	3.35	3.66	0.58
C2R50	65536	2	1.21	0.5	0.12	1.92	-	0.91
C2R40	65536	2	0.75	0.4	0.11	1.43	-	0.85

The dynamical evolution of the models is studied by means of N-body simulations performed with `starlab`. The systems are followed until $T/T_D = 35$, where $T_D = [3\pi/(16G\rho_{90})]^{1/2}$ is the dynamical time associated with the sphere enclosing 90% of the mass of the system. Here the analysis focuses on model C2R90, for details about the other models see [10].

The instabilities are dominated by global m = 1, 2 modes

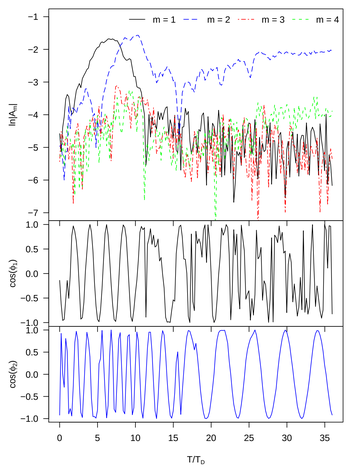

Fig. 1: Fourier analysis of the density of model C2R90. **Top panel:** Growth of the amplitude of the Fourier coefficient $|A_m|$, for $m = 1, 2, 3, 4$. **Bottom panels:** Cosine of the phase angle ϕ_m for the dominant modes $m = 1, 2$.

The instabilities are studied by means of a Fourier analysis of the density distribution of the models. We define the complex coefficient associated with the mode of azimuthal number m as:

$$C_m = \frac{1}{2\pi}\int_0^{2\pi} \rho(R, z, \phi; T)\, e^{-im\phi} d\phi \quad (2)$$

with the normalized coefficient $A_m(R, z; T) = C_m(R, z; T)/C_0(R, z; T)$.

The tangent of the phase angle of the m-th mode is then defined as

$$\phi_m = \tan^{-1}\left[\frac{-\Im(A_m)}{\Re(A_m)}\right] \quad (3)$$

and the associated pattern speed is given by $\sigma_m/m = (\partial\phi_m/\partial T)/m$.

Morphological evolution

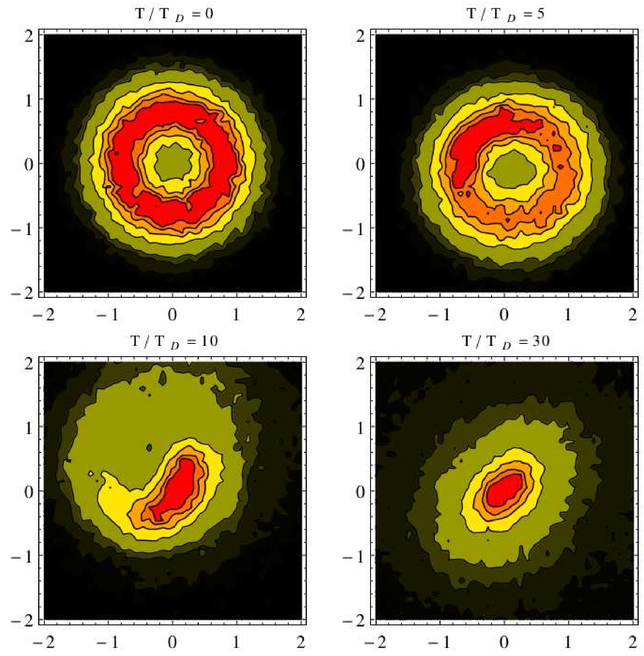

Fig. 2: Time evolution of the surface density of model C2R90, projected on the equatorial plane (x, y). An $m = 1$ (lop-sided) mode emerges by $T/T_D = 5$ and then gives way to an $m = 2$ (bar) mode by $T/T_D = 30$. In each panel, the surface density is normalized to the maximum value; from red to black, the isodensity contours correspond to $\Sigma/\Sigma_{max} = 0.77, 0.65, 0.5, 0.3, 0.1, 0.05, 0.01, 0.001$. Time is expressed in units of the dynamical time and spatial coordinates are in N-body units.

Corotation points appear when modes become unstable

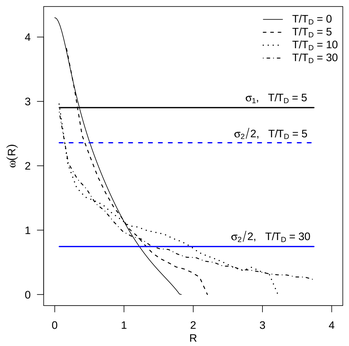

The corotation point is defined as the radial position in the configuration at which the pattern speed of a given mode is equal to the angular velocity of the system $\omega(R_{cor}) = \sigma_m/m$.

From the calculation of the pattern speed of the $m = 1, 2$ modes at different times of the evolution, it appears that the corotation point associated with the $m = 1$ mode disappears almost exactly when the $m = 1$ becomes subdominant with respect to the $m = 2$ mode ($T/T_D \approx 8$).

Fig. 3: Radial profile of the angular velocity of the model C2R90 at different times of the evolution. Thick horizontal lines mark the pattern speeds of the two dominant modes $m = 1, 2$ in the two phases of the evolution.

Curious about the initial equilibria?
See [9] for details!

While in the moderate rotation regime the equilibria are dynamically stable and suited for describing rotating globular star clusters [1], here we focus on the strong differential rotation regime in which the configurations show an off-center density maximum.

Analogies with differentially rotating fluid polytropes

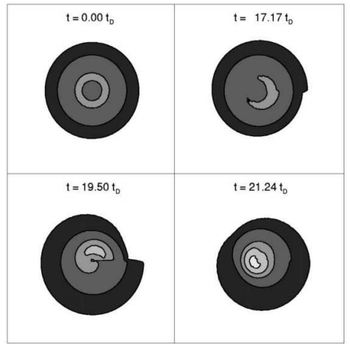

The surprising discovery of an unstable $m = 1$ mode in polytropes with strong differential rotation [2] kindled a revival of interest in the study of stabilities of rotating fluids.

Numerical studies [5] [7] have confirmed that $m = 1, 2$ modes can become unstable in a variety of differentially rotating fluid models, having values of t as low as $t \approx 0.01$ [8].

The study of the stability of differentially rotating spherical shells suggests that the unstable modes are characterized by corotation within the system [11].

The models presented in this study may be interpreted broadly as stellar dynamical counterparts of the fluid systems examined by [2] and [7].

Fig. 4: Time evolution of the isodensity contours in the equatorial plane of a differentially rotating polytropic model with index $n = 3.33$ and $t = 0.14$ (taken from Fig. 2 in [2]).

The role of the degree of differential rotation

Too simplistic to describe the emergence of dynamical instabilities in rotating stellar systems by means of the parameter t alone!

We further investigated the role of the degree of differential rotation by means of an additional series of N-body simulations.

The initial configurations are characterized by a King (1966) density distribution with $\Psi = 7$ in which the "j-constant" rotation law is introduced

$$\omega(R) = \omega_c A^2/(A^2 + R^2) \quad (4)$$

where R is the cylindrical radius and $A = R_{90}/n$.

The degree of differential rotation is measured by $d = n^2 + 1$. The global amount of rotation is measured by t (t_{eff} denotes the value of t after a short initial transient phase).

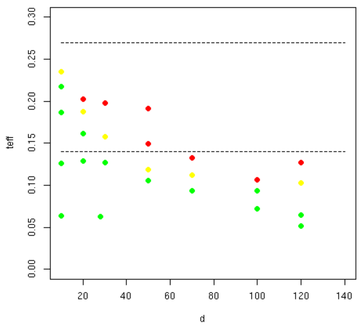

Fig. 5: Green, yellow, and red dots denote stable, marginally stable, and unstable configurations, respectively. Dashed lines mark the critical values ($t = 0.14, 0.27$) for dynamical instability according to [4] and the sequence of Maclaurin ellipsoids (e.g., see [3]).

ALV thanks D. C. Heggie for discussions and the Royal Commission for the Exhibition of 1851 and The Gruber Foundation for support. GB is partially supported by the Italian MIUR.

Animations!
http://alvarri.com/dyninstab
Questions?
annalisa.varri@gmail.com
@parallasseh

References

[1] Bianchini, P., Varri, A. L., et al. 2013, ApJ, 772, 67
[2] Centrella, J. M. et al. 2001, ApJL, 550, L193
[3] Chandrasekhar, S. 1969 Ellipsoidal Figures of Equilibrium, Yale Univ. Press
[4] Ostriker, J. P. & Peebles, P. J. E. 1973, ApJ, 186, 467
[5] Ou, S. & Tohline, J. E. 2006, ApJ, 651, 1068
[6] Portegies Zwart, S. F., et al. 2001, MNRAS, 321, 199
[7] Saijo, M., et al. 2003, ApJ, 595, 352
[8] Shibata, M., et al. 2002, MNRAS, 334, L27
[9] Varri, A. L., & Bertin, G. 2012, A&A, 540, A94
[10] Varri, A. L., Vesperini, E. et al. ApJ submitted
[11] Watts, A. L., et al. 2005, ApJL, 618, L37